

Droplet impact on a dry surface: triggering the splash with a small obstacle

By C. JOSSERAND¹, L. LEMOYNE², R. TROEGER²
AND S. ZALESKI¹

¹Laboratoire de Modélisation en Mécanique, case 162, 4 place Jussieu, 75005 Paris, France

²Laboratoire de Mécanique Physique, 2 pce. gare de ceinture, 78210 St. Cyr, France,
jossieran@lmm.jussieu.fr

(Received 22 October 2003 and in revised form 9 September 2004)

Droplet impact on a dry solid surface is investigated experimentally. A small obstacle made by layers of adhesive tape is located on the solid surface at some distance from the impact centre. The splashing of the drop starts at the tape, as a sheet of liquid shoots upwards. Angle, speed and dynamics of this liquid sheet are investigated as a function of the distance from the impact centre to the obstacle and its height. Reynolds and Weber numbers are kept constant. Volume-of-fluid simulations reproduce the experiments qualitatively. Measured sheet angles are compared with the predictions of a simple theory.

1. Introduction

Splashing, corolla crown formation, and jets are well-known features of droplet impacts. Famous photographs (Edgerton & Killian 1954; Worthington 1876) and everyday-life situations have popularized these phenomena. Droplet impact, though being an old and almost classical problem, has benefited from numerous recent studies enhanced by both the improvement of visualization and experimental techniques and by the tremendous development of numerical techniques and power (Stow & Hadfield 1981; Yarin & Weiss 1995; Cossali, Coghe & Marengo 1997; Gueyffier & Zaleski 1998; Rieber & Frohn 1998; Weiss & Yarin 1999; Bussmann, Chandra & Mostaghimi 2000; Wang & Chen 2000; Davidson 2000; Rioboo, Marengo & Tropea 2001; Thoroddsen 2002; Roisman & Tropea 2002; Josserand & Zaleski 2003). Fluid impacts appear in various contexts and many technological applications. Examples include ink-jet printing (Chaudhary & Maxworthy 1980; Wallace 2001), sea-wave impacts (Cooker & Peregrine 1995), and coating processes (Oğuz & Prosperetti 1990). Splashing and spreading also correspond to a dramatic change in the topological structures of the free-surface flow after impact. Understanding the transition from one to the other is of fundamental importance for our knowledge of such flows (Peregrine 1981; Rein 1993).

Consider the simple case of a vertical droplet impact on a horizontal dry solid surface. Depending on the parameters one can observe a large variety of results (Rioboo *et al.* 2001). For instance, low surface tension and low viscosity (large Weber and Reynolds numbers) promote splash, secondary droplet breakup and/or corolla formation. On the other hand, a high viscosity (low Reynolds number) can suppress the splash and only droplet deposition is observed. Similarly, the solid-surface properties have an effect on the formation of splashes. In particular, experiments

have shown that the rougher the solid, the more likely it is that the droplet splashes (Rioboo *et al.* 2001). The investigation of this as yet unexplained effect motivated the present work. Spreading is sought for good ink-jet printing but splashes are desirable in combustion chambers for instance. Thus, the understanding and control of this splashing/spreading transition are needed both from a fundamental and a practical point of view. When only capillarity and viscosity are considered, experimental laws have been obtained for both dry and wet surfaces (Mundo, Sommerfeld & Tropea 1995). They involve the dimensionless splashing parameter $K = We^{1/2} Re^{1/4}$. The critical value K_c that separates spreading from splashing behaviour depends on other experimental parameters. For impacts on thin liquid films (Yarin & Weiss 1995; Josserand & Zaleski 2003) K_c depends on the dimensionless ratio between the droplet radius and the liquid layer thickness. For impacts on dry surfaces (Rioboo *et al.* 2001) K_c depends on the surface roughness.

The present study is an attempt to understand this last dependence through a model experiment. We describe the impact of a droplet on a smooth solid surface with a single step change of the surface elevation. This localized surface fluctuation forms an obstacle which deviates the rapidly spreading liquid layer. In this first approach, we focus on the phenomenological description of the dynamics since we restrict our presentation to a single choice of Reynolds and Weber numbers. A few numerical and experimental studies have recently been devoted to drop impact on non-flat surfaces: some are in the context of molten-metal droplet impact (Liu, Lavernia & Rangel 1995; Ghafouri-Azar *et al.* 2003) while another considers controlled surface roughness (Range & Feuillebois 1998). For molten-metal droplet impact, the surface fluctuation is created by the preceding impacting droplet. Although we observe splashing results similar to those of Ghafouri-Azar *et al.* (2003), for molten droplets the dynamics is more complex to analyse since the obstacle geometry is not controlled at all, leaving aside the temperature field and phase transition influences. In the other studies the surface fluctuations were controlled, either by the addition of grooves on the flat surface (Range & Feuillebois 1998) or by considering numerical simulations of drop impact on periodically perturbed surfaces (Liu *et al.* 1995).

2. Experimental setup

Images of impacting droplets are obtained with a classical droplet generator and experimental facility. Experiments are performed with demineralized water. Droplets fall from a precision syringe with a diameter $D = 3.7$ mm and impact a plate at speed $U = 3.3$ m s⁻¹. The Reynolds $Re = UD/\nu = 12200$ and Weber number $We = \rho U^2 D / \sigma = 514$ are fixed throughout the experiments. The Froude number, the ratio between gravity force and inertia $Fr = gD/U^2$, value of 0.0037 shows that gravity can be neglected during the impact dynamics. Droplets prior to impingement were observed and the sphericity verified (diameter distortion is less than 10%).

The plate is made of inox coated with Teflon in order to avoid wetting as much as possible. An obstacle is set in the path of the spreading droplet by one or several layers of adhesive tape. The height of the obstacle is controlled by the number of layers and the distance between the obstacle and the impact point is measured by a micrometer table. Each layer of tape is 0.035 ± 0.002 mm thick and is placed orthogonally to the observation plane. The obstacle is therefore non-axisymmetrical. The impact plate offers a very smooth surface ($Ra < 0.5$ μ m, Ra being the arithmetical mean roughness and measured before Teflon coating) and its temperature is controlled at 25 °C. Pictures are obtained with a Stanford Optics intensified CCD camera triggered



FIGURE 1. Impact on the 0.035 mm obstacle (from left to right 1000, 1500 and 1750 μs after impact). A sketch of the measurement of the angle of deviation is shown on the right-hand figure.



FIGURE 2. Impact on the 0.07 mm obstacle (from left to right: 1000, 1500, 2000 μs after impact).

by a light barrier consisting of a laser diode opposite a photomultiplier. This solution has been retained in order to obtain maximum repeatability of camera triggering. The triggering is adjusted on the decreasing rate of the photomultiplier signal. Backlighting is obtained with a Spectra Physics 355 nm Argon laser at 300 mW diffused by acid-polished glass. A specific micro-telescope is mounted on the camera allowing a 1 cm area to be observed. In order to observe small-scale features of the splashing on an obstacle, time exposure has been lowered to 2 μs . Different steps of the impact process are obtained by controlling the delay of camera triggering with the photomultiplier gate. Velocity measurements during impact are verified by multi-exposure images (not shown here). Repeatability of the overall imaging procedure is improved by manually eliminating obviously failed images, mostly due to parasite light triggering the photomultiplier. Considering the different error sources, we estimate the error made in diameter and velocity measurements at 2%, whereas the error made in other values (such as angles and liquid thicknesses) is 5%. Rioboo (2001) gives detailed error estimates for a very similar experimental setup. Although repeatability has been a permanent concern in developing the experimental setup, each time step of impact is repeated until three almost identical features are obtained.

3. Results and discussion

Three series of impacts with an obstacle are shown for obstacle thicknesses $e = 0.035$, 0.07 and 0.2 mm. The distance d_{obs} between the impact point of the droplet and the obstacle has been varied, from 0 to 4.5 mm. In figures 1 to 3, different stages of impact and splashing are shown.

Figure 1 pictures a droplet falling on a plate with a 0.035 mm-high obstacle placed 2 mm from the droplet impact centre. Figure 2 shows a droplet falling on a plate with an obstacle 0.07 mm high placed closer to the centre. Last, figure 3 shows a droplet



FIGURE 3. Impact on the 0.2 mm obstacle (from left to right: 1000, 1500, 2500 μ s after impact).

falling on a plate with an obstacle 0.2 mm high at a distance similar to the previous one. Time $t=0$ is when the droplet touches the plate (not the obstacle).

The onset of a splash when the droplet arrives on the obstacle is clearly seen in these figures. The angle, width and velocity of the liquid sheet that shoots up upon impact vary with the distance from the impact centre to the obstacle and the height of the obstacle. Figures 1, 2 and 3 also indicate that the higher the obstacle, the more vertical the liquid sheet will be. In figure 4(a), sheet angles are plotted against time. In a first phase of the interaction of the jet with the obstacle the liquid is ejected almost vertically. The liquid sheet fed by the spreading film develops as the deviation angle decreases, apparently asymptoting a steady state.

In figure 4(b) this stabilized apparent angle of the liquid sheet is plotted against the dimensionless (by droplet diameter) obstacle position for a 0.07 mm thick layer. The plotted angle is that between the median straight line of the liquid sheet and the obstacle plate. A sketch of this measured angle is superimposed on the experimental photograph in figure 1. When the droplet falls directly on the obstacle (distance of droplet impact point to obstacle is less than droplet radius) no splash is observed (angle 0°). When the splash occurs, the direction of the liquid sheet is more vertical when the impact is closer to the obstacle. In fact, if an encounter with the obstacle happens in the early stages of spreading, the liquid film seems to be projected vertically, whereas when the obstacle is met at the end of spreading, the liquid film only climbs over the obstacle. This may result from different thicknesses of the liquid film at different stages of spreading, confirming a theoretical prediction made by Josserand & Zaleski (2003) and discussed in §5 below, that the film becomes thicker as time advances. This is a rather difficult fact to verify experimentally with an acceptable precision.

Liquid sheet length can be measured as the distance from the obstacle position to the point where filaments appear at the upper end (figure 5). Its evolution with time shows that the liquid sheet has an almost-constant velocity. This interesting feature may be explained as follows. First, when the film is ejected from the droplet, theory predicts that this happens at a constant velocity (Josserand & Zaleski 2003). Second, after ejection the velocity is mostly conserved: we use Teflon-coated plates, which are non-wetting. Thus, the singular viscous dissipation near the contact line is avoided. With little dissipation, the velocity remains constant. Moreover we have observed that the sheet thickness remains roughly constant throughout the explored time span, at around 0.5 mm for obstacles of height 0.035 and 0.07 mm, and at 0.7 mm for the 0.2 mm obstacle.

Secondary droplet formation is enhanced by shorter distances from the obstacle as less momentum is dissipated between the instant of impact on the plate and the instant of first contact with the obstacle. Also, large obstacles enhance secondary droplet formation. When plotting on the same image the droplet contours during

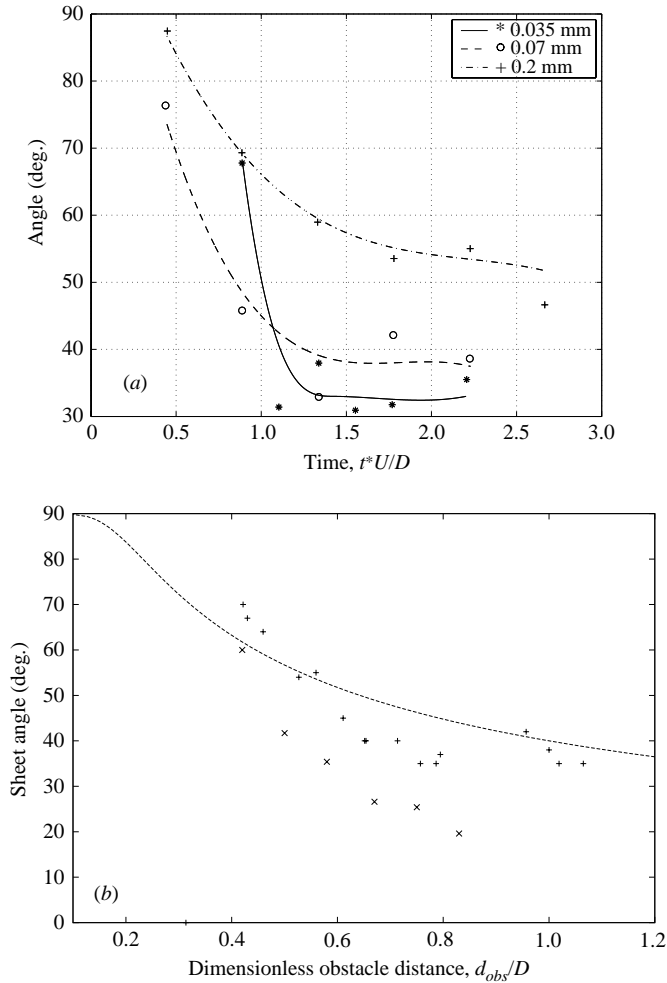


FIGURE 4. (a) Angle of liquid sheet versus dimensionless time. (Symbols represent experimental measurements, lines represent their interpolation.) (b) Angle of liquid finger versus the dimensionless obstacle distance. +, experimental values; ---, theoretical prediction; ×, numerical simulation results.

impact, we observe that with the smaller obstacle (figure 6a), the sheet develops to a greater length than with the medium size obstacle (figure 6b). One may also notice the difference between the centre figure (figure 6b 0.07 mm obstacle) and the left and right figures (0.035 figure 6a and 0.2 mm figure 6c): the base of the sheet seems fixed for the 0.035 and 0.2 mm cases whereas it advances over the obstacle with finger development for the 0.07 mm case.

4. Numerical simulation

We now compare the dynamics observed in the experiments with numerical simulations of axisymetrical drop impacts. We use here a volume-of-fluid (VOF) numerical scheme already used by two of us for the study of droplet impacts on thin liquid layers (Josserand & Zaleski 2003).

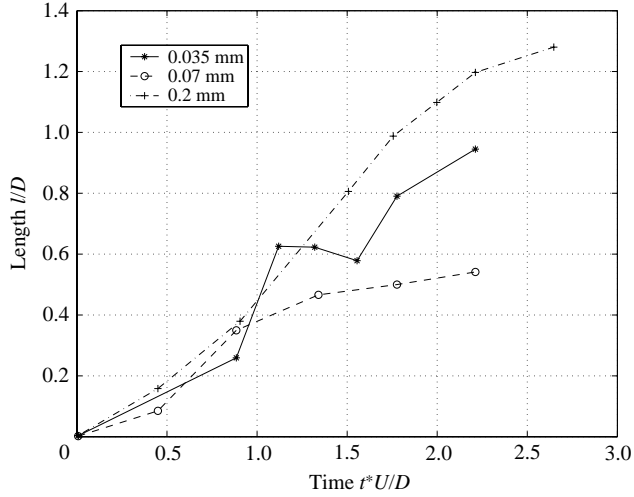
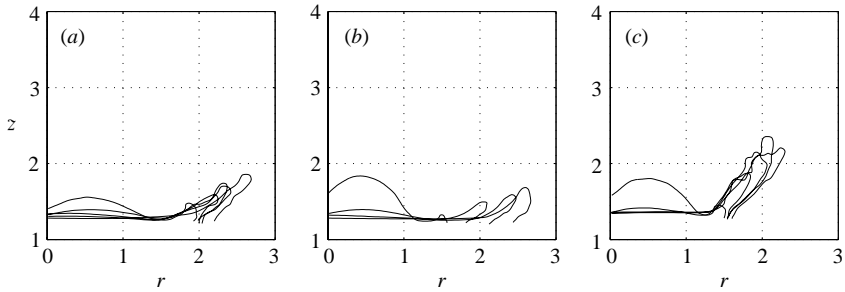


FIGURE 5. Dimensionless length of the liquid sheet versus dimensionless time.

FIGURE 6. Droplet contours at various times for (a) $e=0.035$ mm, (b) $e=0.07$ mm and (c) $e=0.2$ mm. Distances are made dimensionless by droplet diameter.

The main additional difficulties in modelling drop impact on a solid surface arise at the moving contact line. This contact line is located at the boundary between gas, liquid and solid. It still poses a hard challenge for theory and modelling (de Gennes 1985). In particular, the equations of hydrodynamics lead to a stress singularity near the moving contact line (Dussan V. & Davis 1974). This mathematical singularity can be avoided through still-debated physical cut-off prescriptions (de Gennes 1985; Oron, Davis & Bankoff 1997; Shikmurzaev 1993) but researchers lack as yet a full understanding of the dynamics there.

For numerical simulations, a major concern is to suppress this unphysical singularity. The few numerical simulations that have been reported in the literature mostly involve a wall-slip condition, which suppresses in particular the moving contact line singularity (Pasandideh-Fard *et al.* 1996; Bussmann *et al.* 2000; Renardy, Renardy & Li 2001; Renardy *et al.* 2003; Reznik & Yarin 2002).

We solve the Navier–Stokes equation for axisymmetric incompressible flow with surface tension written in the one-fluid formulation

$$\rho \left(\frac{\partial \mathbf{u}}{\partial t} + \mathbf{u} \cdot \nabla \mathbf{u} \right) = -\nabla p + \mu \Delta \mathbf{u} + \sigma \kappa \delta_s \mathbf{n}, \quad (4.1)$$

where \mathbf{u} is the fluid velocity, ρ the fluid density and p the pressure. The vector \mathbf{n} denotes the normal to the interface, σ is the surface tension and δ_s the delta function restricted to the interface. Gravity is neglected since the Froude number is the same as for the experiments. The continuity equation is

$$\nabla \cdot \mathbf{u} = 0. \quad (4.2)$$

The discretization is performed on a marker-and-cell (MAC) grid and pressure is solved by the explicit projection method making use of multigrid convergence. The interface is followed by the volume-of-fluid/piecewise-linear-interface-calculation (VOF/PLIC) method of Li (1995) and the capillary force is computed through a variant of the continuous surface stress and continuous surface force methods (Lafaurie *et al.* 1994; Scardovelli & Zaleski 1999; Gueyffier *et al.* 1999) adapted to axisymmetric geometry. A full description of the method can be found in (Gueyffier *et al.* 1999) except for the adaptation to axisymmetric geometry which is described in Gueyffier (2000).

The additional obstacle layer is made circular here for numerical convenience (axisymmetry) while experiments were made with straight adhesive tape. Boundary conditions are crucial for the modelling. On the solid wall we impose a no-slip condition $\mathbf{u} = 0$, and Neuman conditions are taken for the colour function: the derivative in the direction normal to the solid vanishes, i.e. $\partial c / \partial n = 0$. This boundary condition imposes a constant contact angle of 90° which corresponds to intermediate wetting. Surprisingly, we have observed numerically that this boundary condition coupled with the no-slip condition results in no singular viscous dissipation near the moving contact line. The numerical discretization acts here as a sufficient cut-off.

These conditions are now applied for all the solid boundaries including the obstacle. However to simplify the writing of the code, the $\mathbf{u} \cdot \mathbf{n} = 0$ boundary condition is not applied during the projection step, i.e. the Poisson equation for the pressure is solved with a flat boundary instead of the obstacle. The pressure field is thus not accurately solved near the obstacle and local mass conservation may not be satisfied: a zero mass flow across the obstacle is not imposed. However in the simulations reported below the mass loss during the runs is less than 5%.

These numerical simplifications have made quantitative comparisons between experiments and numerics hard to obtain. In particular, we emphasize that the difference between our axisymmetric numerics and the straight experimental configuration should be relevant at small distance only. For fluid parameters (densities, viscosities, surface tension) similar to the experimental values, the thickness of the spreading film was found much thinner than in experiments. Such a discrepancy, probably due to the absence of roughness at the idealized wall surface, leads to very different dynamics since the liquid sheet splashes promptly at the obstacle and breaks up into tiny droplets. To avoid this effect and to increase the numerical film thickness, we have used a higher liquid viscosity. Moreover, the gas density was taken twice higher than the air density in order to diminish numerical instabilities due to high density ratio. With these restrictions, we have performed numerical simulations for physical parameters as close as possible to the experimental value: drop diameter $D = 3.6$ mm, liquid density that of water, surface tension $\sigma = 0.07$ SI, so that the Weber number $We = 514$ is equal to that of the experiment while the Reynolds number $Re = 2400$ is 5 times smaller. The step height is 0.07 mm. Figure 7 shows snapshots of the impact dynamics for a distance of the obstacle from the impact centre of $d_{obs} = 0.66D$.

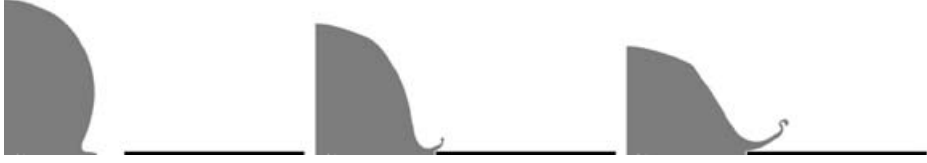


FIGURE 7. Numerical simulation of droplet impact for $We = 514$, $Re = 2400$ and $d_{obs}/D = 2/3$. The figures show the density profiles at times 200, 400 and 600 μs after impact.



FIGURE 8. Deviated liquid jet of impacting drops with $We = 514$, $Re = 2400$ and varying obstacle distance; $d_{obs}/D = 0.4, 0.58$ and 0.83 from left to right.

We retrieve the general features of the experiments: splashing appears at the obstacle and generates a deviated liquid sheet. The deviation of the liquid is initially almost vertical, then converges to an almost constant angle. We have also varied the obstacle distance from the impact centre as shown on figure 8. We notice again that increasing the obstacle distance decreases the liquid deviation as observed experimentally. Moreover, the angles of deviation for the different ratios d_{obs}/D computed numerically have been drawn on figure 4(b) for qualitative comparisons. The angles from the numerics are systematically smaller than those observed in experiments, but the general trend of the dependence on the ratio d_{obs}/D is retrieved.

5. Theory

We want to study the jet–obstacle interaction in a simplified framework and so consider two-dimensional geometry. We explore the steady flow of a jet of height h , speed U along an horizontal surface encountering a step change e of the surface elevation and thus deviated by an angle α from the horizontal axis. The Reynolds number is considered high enough so that the influence of viscosity can be neglected in the first approximation. In writing momentum conservation in a region enclosing the step we find

$$u^2 h = u^2 h \cos \alpha + \int_0^e p \, dy. \quad (5.1)$$

Without viscosity, the pressure must scale with ρu^2 . From Bernoulli's theorem it is $\rho u^2/2$ in the bottom corner below the step at $y=0$. The condition $p=0$ holds on the free surface and thus $p=0$ also at the top corner at $y=e$ where the free surface starts. Thus it is reasonable to assume that p interpolates between these two values, in a way that weakly depends on α . This leads to

$$\frac{e}{h} = C''(1 - \cos \alpha), \quad (5.2)$$

where C'' is a dimensionless numerical constant, depending on α . It is possible to verify (5.2) by direct numerical simulation (results obtained with R. Scardovelli and S. Popinet will be published elsewhere). Although a potential flow theory exists

(Birkhoff & Zarantonello 1957), there is no certainty that the actual flow is potential and preliminary results from numerical simulations seem to indicate that it is not, but that a relation of the form (5.2) does hold.

Going back to the full problem, we identify h with the thickness of the rapidly expanding film, which is difficult to determine. However a simple estimate can be made as follows. It has been argued by two of us (Josserand & Zaleski 2003) that the thickness of the jet is of the order $h \simeq C\sqrt{\nu t}$ where t is the time from drop impact, and C is a dimensionless constant. Such a scaling was initially introduced by Yarin & Weiss (1995) where the time was taken as the impact frequency of a train of droplets. Estimating t here as the inertial time $t \sim d_{obs}/U$ we obtain

$$h \simeq C\sqrt{\nu d_{obs}/U}. \quad (5.3)$$

We choose C as a fitting parameter and obtain from (5.3) and (5.2) the dashed line in figure 4(b). The general trend is in agreement with the experiment but there is obviously room for improvement: more refined estimates for h could be made for instance.

To summarize, we have observed the triggering of a splash by a small obstacle. Numerical simulations are in qualitative agreement and show similar dependence of the dynamics on the distance of the obstacle from the impact centre. A simple potential flow model also reproduces the trend observed in the experiments. However more refined studies, both experimental and theoretical, are needed to determine the thickness of the spreading layer. The present study could also be expanded to investigate splashes on a rough surfaces, modelling the roughness as a collection of small obstacles.

REFERENCES

- BIRKHOFF, G. & ZARANTONELLO, E. 1957 *Jets, Wakes and Cavities*. Academic.
- BUSSMANN, M., CHANDRA, S. & MOSTAGHIMI, J. 2000 Modeling the splash of a droplet impacting a solid surface. *Phys. Fluids* **12**, 3121–3132.
- CHAUDHARY, K. C. & MAXWORTHY, T. 1980 The nonlinear capillary instability of a liquid jet. Part 3. Experiments on satellite drop formation and control. *J. Fluid Mech.* **96**, 287–297.
- COOKER, M. & PEREGRINE, D. 1995 Pressure-impulse theory for liquid impact problems. *J. Fluid Mech.* **297**, 193–214.
- COSSALI, G., COGHE, A. & MARENGO, M. 1997 The impact of a single drop on a wetted solid surface. *Exps. Fluids* **22**, 463–472.
- DAVIDSON, M. 2000 Boundary integral prediction of the spreading of an inviscid drop impacting on a solid surface. *Chem. Engng Sci.* **55**, 1159.
- DUSSAN V., E. & DAVIS, S. 1974 On the motion of a fluid-fluid interface along a solid surface. *J. Fluid Mech.* **65**, 71–95.
- EDGERTON, H. & KILLIAN, J. 1954 *Flash*. Boston: Branford.
- DE GENNES, P. 1985 Wetting: statics and dynamics. *Rev. Mod. Phys.* **57**, 827.
- GHAFOURI-AZAR, R., SHAKERI, S., CHANDRA, S. & MOSTAGHIMI, J. 2003 Interaction between molten metal droplets impinging on a solid surface. *Int. J. Heat Mass Transfer* **46**, 1395–1407.
- GUEYFFIER, D. 2000 Etude de l'impact de gouttes sur un film liquide mince. PhD thesis, Université Pierre et Marie Curie.
- GUEYFFIER, D., NADIM, A., LI, J., SCARDOVELLI, R. & ZALESKI, S. 1999 Volume of fluid interface tracking with smoothed surface stress methods for three-dimensional flows. *J. Comput. Phys.* **152**, 423–456.
- GUEYFFIER, D. & ZALESKI, S. 1998 Formation de digitations lors de l'impact d'une goutte sur un film liquide. *C. R. Acad. Sci. Paris IIb* **326**, 839–844.
- JOSSERAND, C. & ZALESKI, S. 2003 Droplet splashing on a thin liquid film. *Phys. Fluids* **15**, 1650.

- LAFABURIE, B., NARDONE, C., SCARDOVELLI, R., ZALESKI, S. & ZANETTI, G. 1994 Modelling merging and fragmentation in multiphase flows with SURFER. *J. Comput. Phys.* **113**, 134–147.
- LI, J. 1995 Calcul d'interface affine par morceaux (piecewise linear interface calculation). *C. R. Acad. Sci. Paris IIB* **320**, 391–396.
- LIU, H., LAVERNIA, E. & RANGEL, R. 1995 Modeling of molten droplet impingement on a non-flat surface. *Acta Metall. Mater.* **43**, 2053–2072.
- MUNDO, C., SOMMERFELD, M. & TROPEA, C. 1995 Droplet-wall collisions: Experimental studies of the deformation and breakup process. *Intl J. Multiphase Flow* **21**, 151.
- OĞUZ, H. & PROSPERETTI, A. 1990 Bubble entrainment by the impact of drops on liquid surfaces. *J. Fluid Mech.* **219**, 143–179.
- ORON, A., DAVIS, S. & BANKOFF, S. 1997 Long-scale evolution of thin liquid films. *Rev. Mod. Phys.* **69**, 931.
- PASANDIDEH-FARD, M., QIAO, Y., CHANDRA, S. & MOSTAGHIMI, J. 1996 Capillary effects during droplet impact on a solid surface. *Phys. Fluids* **8**, 650.
- PEREGRINE, D. 1981 The fascination of fluid mechanics. *J. Fluid Mech.* **106**, 59–80.
- RANGE, K. & FEUILLEBOIS, F. 1998 Influence of surface roughness on liquid drop impact. *J. Colloid. and Interface Science* **203**, 16–30.
- REIN, M. 1993 Phenomena of liquid drop impact on solid and liquid surfaces. *Fluid Dyn. Res.* **12**, 61.
- RENARDY, M., RENARDY, Y. & LI, J. 2001 Numerical simulation of moving contact line problems using a volume-of-fluid method. *J. Comput. Phys.* **171**, 243–263.
- RENARDY, Y., POPINET, S., DUCHEMIN, L., RENARDY, M., ZALESKI, S., JOSSERAND, C., DRUMRIGHT-CLARKE, M., RICHARD, D., CLANET, C. & QUÉRÉ, D. 2003 Pyramidal and toroidal water drops after impact on a solid surface. *J. Fluid Mech.* **484**, 69–83.
- REZNIK, S. & YARIN, A. 2002 Spreading of an axisymmetric viscous drop due to gravity and capillarity on a dry horizontal wall. *Intl J. Multiphase Flow* **28**, 1437–1457.
- RIEBER, M. & FROHN, A. 1998 *Numerical Simulation of Splashing Drops*. Academic.
- RIOBOO, R. 2001 Impact de gouttes sur surfaces solides et seches. PhD thesis, Université Pierre et Marie Curie.
- RIOBOO, R., MARENGO, M. & TROPEA, C. 2001 Outcomes from a drop impact on solid surfaces. *Atomization Sprays* **11**, 155–165.
- ROISMAN, I. & TROPEA, C. 2002 Impact of a drop onto a wetted wall: description of crown formation and propagation. *J. Fluid Mech.* **472**, 373–397.
- SCARDOVELLI, R. & ZALESKI, S. 1999 Direct numerical simulation of free-surface and interfacial flow. *Annu. Rev. Fluid Mech.* **31**, 567–603.
- SHIKMURZAEV, Y. 1993 The moving contact line on a smooth solid surface. *Intl J. Multiphase Flow* **19**, 586–610.
- STOW, C. & HADFIELD, M. 1981 An experimental investigation of fluid flow resulting from the impact of a water drop with an unyielding dry surface. *Proc. R. Soc. Lond. A* **373**, 419.
- THORODDSEN, S. 2002 The ejecta sheet generated by the impact of a drop. *J. Fluid Mech.* **451**, 373–381.
- WALLACE, D. B. 2001 Ink-jet applications, physics, and modelling – an industrial/applied research view. Talk delivered at IMA “Hot Topics” Workshop: *Analysis and Modeling of Industrial Jetting Processes*, <http://www.ima.umn.edu/multimedia/abstract/1-10abs.html#wallace>.
- WANG, A.-B. & CHEN, C.-C. 2000 Splashing impact of a single drop onto very thin liquid films. *Phys. Fluids* **12**, 2155–2158.
- WEISS, D. & YARIN, A. 1999 Single drop impact onto liquid films: neck distortion, jetting, tiny bubble entrainment, and crown formation. *J. Fluid Mech.* **385**, 229–254.
- WORTHINGTON, A. 1876 On the form assumed by drops of liquids falling vertically on a horizontal plate. *Proc. R. Soc. Lond.* **25**, 261–271.
- YARIN, A. & WEISS, D. 1995 Impact of drops on solid surfaces: self-similar capillary waves, and splashing as a new type of kinematic discontinuity. *J. Fluid Mech.* **283**, 141–173.